Probe Charge-Parity Violation with Axion-Like Particles and Tau Weak Electric Dipole Moments at Future Lepton Colliders

Keping Xie

Tsung-Dao Lee Institute, Shanghai Jiao Tong University

Light ALPs in electroweak channels

CP violation in tau spin observables

New particles and new CP violation at lepton colliders

	Light ALPs	**Tau weak EDMs**
Physics	Pseudoscalar couplings to electroweak gauge bosons	CP-odd $Z\tau\tau$ and $\gamma\tau\tau$ form factors
Observable	Missing energy and hard vector-boson scattering	CP-odd pion angular moments
Collider handle	Tera-Z, e^+e^- at 240/365 GeV, $\mu^+\mu^-$ at 3/10 TeV	Large Z sample and a small off-peak scan

Production kinematics and tau spin retain different information about new physics

ALPs: Bao et al., arXiv:2505.10023. Tau dipoles: Du et al., arXiv:2609.18892 (six-moment revision). The studies use separate collider benchmarks.

Electroweak ALP interactions

A light pseudoscalar with independent mass and interaction scale:

$$-\Delta\mathcal{L} = \frac{a}{f_a}\left(C_B B_{\mu\nu}\widetilde{B}^{\mu\nu} + C_W W^I_{\mu\nu}\widetilde{W}^{I\mu\nu}\right).$$

After electroweak symmetry breaking,

$$-\Delta\mathcal{L} \supset \frac{a}{4}\left(g_{a\gamma\gamma}F\widetilde{F} + g_{a\gamma Z}F\widetilde{Z} + g_{aZZ}Z\widetilde{Z} + g_{aWW}W\widetilde{W}\right).$$

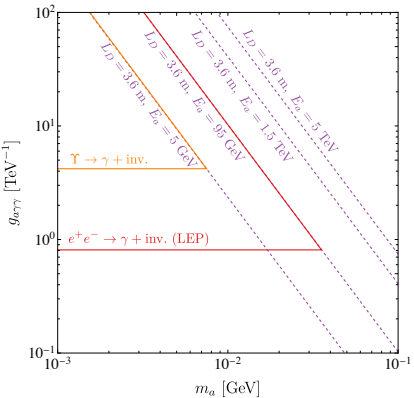
$$g_{a\gamma\gamma} = \frac{4}{f_a}(s_W^2 C_W + c_W^2 C_B),$$
$$g_{a\gamma Z} = \frac{8}{f_a}s_W c_W (C_W - C_B).$$

Different final states constrain different directions in (C_B, C_W)

Plot coordinates $C_i\,[f_a/\mathrm{TeV}]$ mean $C_i/(f_a/\mathrm{TeV})$.

Bao, Ma, Wu, Xie and Zhang, arXiv:2505.10023.

ALP lifetime selects the search channel



$$\Gamma(a \to \gamma\gamma) = \frac{g_{a\gamma\gamma}^2 m_a^3}{64\pi}, \qquad \ell_a = \beta\gamma c\tau_a.$$

Escape from the detector

- ℓ_a exceeds the detector scale.
- $\ell^+\ell^- \to a + \gamma/Z$ gives a mono-V signal.

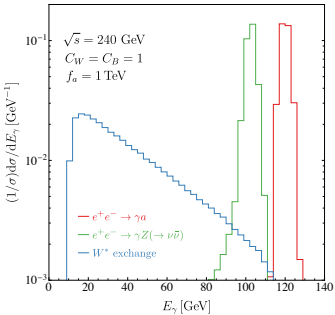
Virtual ALP exchange

- Nonresonant $VV \to VV$ probes $m_a^2 \ll \hat{s}$.
- Sensitivity does not require an observed ALP decay.

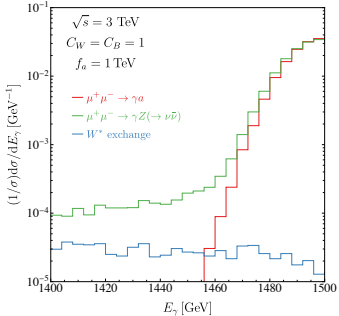
Bao, Ma, Wu, Xie and Zhang, arXiv:2505.10023.

Mono-photon kinematics and detector resolution

e^+e^- **at 240 GeV**



$\mu^+\mu^-$ **at 3 TeV**



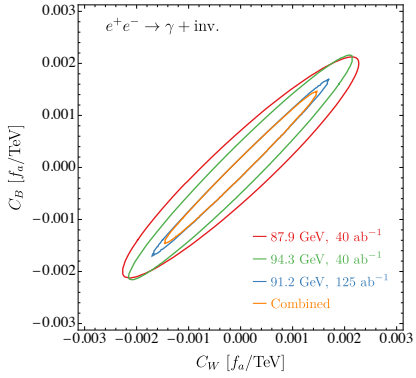
$$E_\gamma = \frac{s - m_a^2}{2\sqrt{s}}, \qquad m_{\rm rec}^2 = s - 2\sqrt{s}\, E_\gamma.$$

At TeV energies, detector smearing merges the light-ALP and $Z \to \nu\bar{\nu}$ peaks.

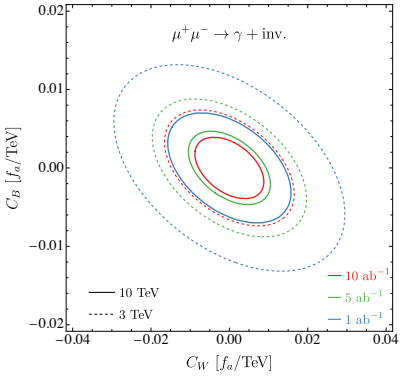
Bao, Ma, Wu, Xie and Zhang, arXiv:2505.10023.

Mono-photon reach at a Z factory and a muon collider

Tera-Z: three running energies



Muon colliders: 3 and 10 TeV

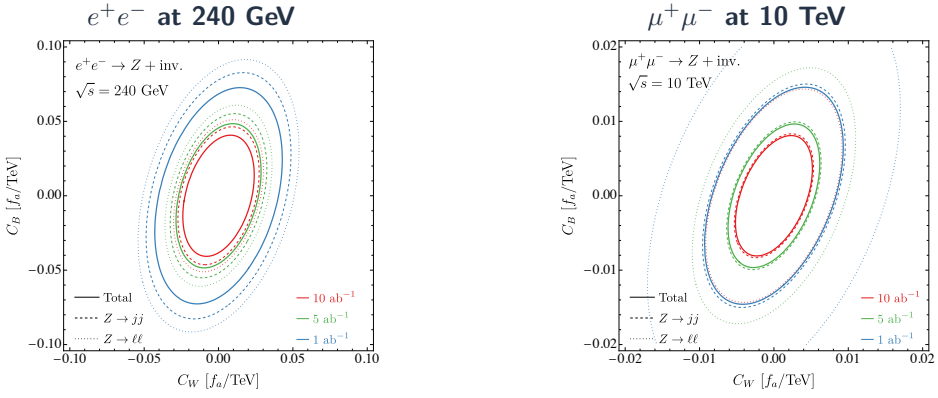


Large Z statistics and smaller high-energy backgrounds both improve reach

Tera-Z: $(87.9, 91.2, 94.3)$ GeV with $(40, 125, 40)\,\text{ab}^{-1}$.

Bao, Ma, Wu, Xie and Zhang, arXiv:2505.10023.

Mono-Z provides complementary coupling information

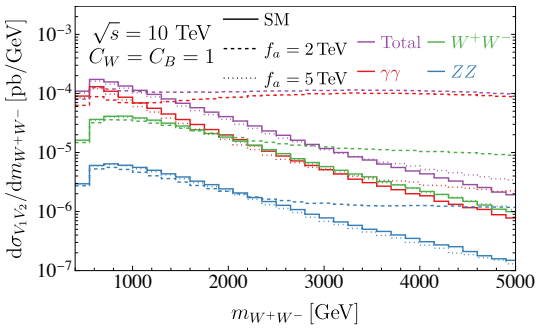


- Reconstruct $Z \to \ell^+\ell^-$ or a hadronic Z and require missing momentum.
- The larger hadronic branching fraction improves reach. At TeV energies, a boosted Z forms a collimated jet.

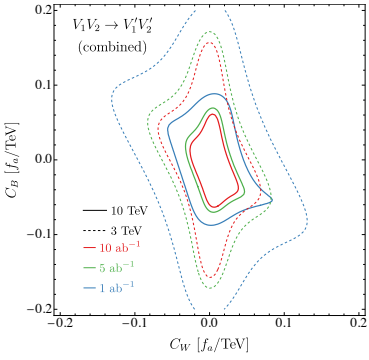
Bao, Ma, Wu, Xie and Zhang, arXiv:2505.10023.

Nonresonant vector-boson scattering probes hard tails

WW invariant mass at 10 TeV



Combined electroweak VBS constraints

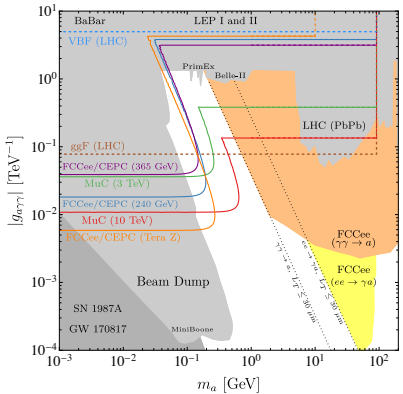


- Derivative ALP interactions enhance the high-energy tail relative to the SM.
- Weak-boson channels probe $g_{a\gamma Z}$, g_{aZZ} and g_{aWW} without requiring an ALP decay.

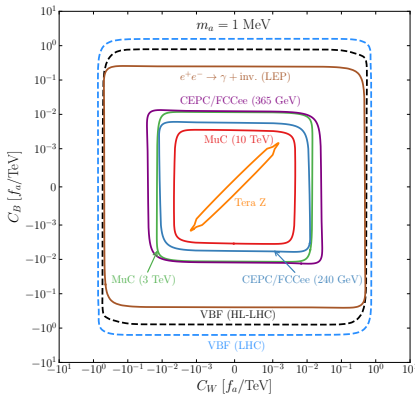
Bao, Ma, Wu, Xie and Zhang, arXiv:2505.10023.

ALP mass and lifetime determine the strongest channel

$|g_{a\gamma\gamma}|$ **versus** m_a



$m_a = 1$ **MeV: electroweak coefficient plane**



Missing energy covers long lifetimes. Virtual exchange extends the mass coverage

Bao, Ma, Wu, Xie and Zhang, arXiv:2505.10023.

Tau dipoles test new CP violation

The tau lifetime makes collider production and decay the route to its dipoles.

$$\Gamma_Z^\nu = ie\left[v_\tau\gamma^\nu - a_\tau\gamma^\nu\gamma^5 + \frac{\widetilde{d}_\tau^W}{2m_\tau}\gamma^5\sigma^{\nu\rho}q_\rho\right].$$

$$\Gamma_\gamma^\nu = ie\left[Q_\tau\gamma^\nu + \frac{\widetilde{d}_\tau^\gamma}{2m_\tau}\gamma^5\sigma^{\nu\rho}q_\rho\right].$$

- $\widetilde{d}_\tau^W$ and $\widetilde{d}_\tau^\gamma$ are dimensionless, complex timelike form factors.
- A joint measurement separates weak and electromagnetic CP violation.
- In dimensionful units, $d_\tau^{W,\gamma} = e\widetilde{d}_\tau^{W,\gamma}/(2m_\tau)$.

10^{-6} in $\widetilde{d}_\tau$ corresponds to $5.552 \times 10^{-21}\, e\,\mathrm{cm}$

Du, Zou, He and Xie, arXiv:2609.18892. Six-moment results from the manuscript revision.

Pion directions analyze tau spin

$$e^-(p_1)e^+(p_2) \to \gamma^*, Z \to \tau^-(k_-)\tau^+(k_+), \qquad \tau^\mp \to \pi^\mp \nu.$$

The two-body pion mode has spin-analyzing power $\alpha_\pi = 1$.

$$\hat{z} = \hat{k}_-, \qquad \hat{y} = \frac{\hat{p}_1 \times \hat{k}_-}{|\hat{p}_1 \times \hat{k}_-|}, \qquad \hat{x} = \hat{y} \times \hat{z}.$$

Longitudinal $\hat{z}$	Along the τ^- flight direction
In-plane $\hat{x}$	Transverse within the production plane
Normal $\hat{y}$	Perpendicular to the production plane

Measure both pion directions in their parent rest frames using one common triad

Du, Zou, He and Xie, arXiv:2609.18892. Six-moment results from the manuscript revision.

Six CP-odd moments and their analytical responses

$$\boldsymbol{L} = \hat{\ell}^- + \hat{\ell}^+, \qquad c = \cos\theta, \qquad \langle \mathcal{O}_i \rangle_Z = -\frac{\beta}{\Delta_0} R_i.$$

Moment	Angular projection	R_i for pure-Z exchange
$\mathcal{O}_1$	L_z	$\frac{4}{3} v_\tau \ \mathrm{Im}\, \widetilde{d}_\tau^W$
$\mathcal{O}_2$	$(\hat{\ell}^- \times \hat{\ell}^+)_z$	$\frac{4}{9} v_\tau \ \mathrm{Re}\, \widetilde{d}_\tau^W$
$\mathcal{O}_3$	L_x	$\frac{\pi}{2} h a_\tau A_e \beta \ \mathrm{Im}\, \widetilde{d}_\tau^W$
$\mathcal{O}_4$	$\mathrm{sgn}(c) L_y$	$\frac{2}{3} h a_\tau \beta \ \mathrm{Re}\, \widetilde{d}_\tau^W$
$\mathcal{O}_5$	L_y	$\frac{\pi}{2} h v_\tau A_e \ \mathrm{Re}\, \widetilde{d}_\tau^W$
$\mathcal{O}_6$	$\mathrm{sgn}(c) L_x$	$\frac{2}{3} h v_\tau \ \mathrm{Im}\, \widetilde{d}_\tau^W$

$$h = m_Z/(2m_\tau), \qquad \beta = \sqrt{1 - h^{-2}}, \qquad A_e = 2v_e a_e/(v_e^2 + a_e^2),$$
$$\Delta_0 = 2a_\tau^2 \beta^2 + v_\tau^2 (3 - \beta^2).$$

At $s = m_Z^2$, linear in $\widetilde{d}_\tau^W$, full angular acceptance and $\alpha_\pi = 1$.

Du, Zou, He and Xie, arXiv:2609.18892. Six-moment results from the manuscript revision.

Transverse moments recover the dipole interference

SM and dipole amplitudes favor different tau helicities. Transverse spin retains their coherence.

$$\frac{\partial\langle\mathcal{O}_4\rangle/\partial\,\mathrm{Re}\,\tilde{d}_\tau^W}{\partial\langle\mathcal{O}_2\rangle/\partial\,\mathrm{Re}\,\tilde{d}_\tau^W} = \frac{3}{2}\frac{m_Z}{2m_\tau}\frac{\beta|a_\tau|}{|v_\tau|} = 521.$$

$$521 = \underbrace{25.7}_{\text{helicity factor}} \times \underbrace{13.5}_{|a_\tau/v_\tau|} \times \underbrace{1.50}_{\text{angular integral}} .$$

- The $\mathrm{sgn}(\cos\theta)$ weight keeps the axial term that cancels on symmetric integration.
- The in-plane response ratio is $\mathcal{O}_3/\mathcal{O}_1 = 60.1$.

These ratios compare the specified moments. They do not represent gains over ALEPH's full analysis.

Du, Zou, He and Xie, arXiv:2609.18892. Six-moment results from the manuscript revision.

Photon–Z interference requires a joint fit

At the pole, the propagator ratio supplies a relative phase:

$$\frac{D^\gamma}{D^Z} = \frac{s - m_Z^2 + i m_Z \Gamma_Z}{s}, \qquad \left.\frac{D^\gamma}{D^Z}\right|_{s=m_Z^2} = 0.0274\, i.$$

The leading transverse responses include

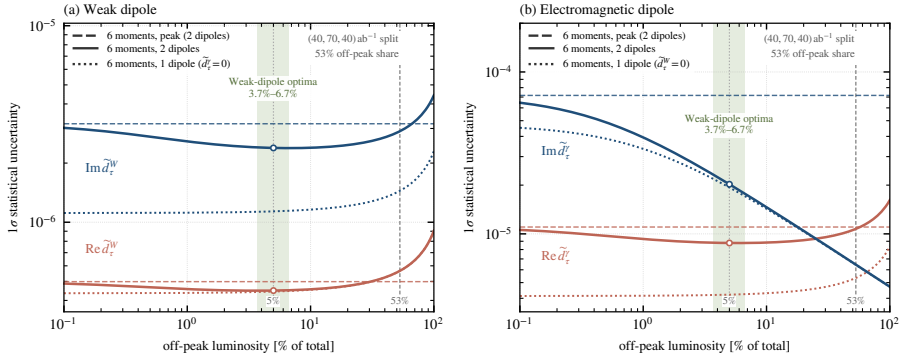
$$\langle \mathcal{O}_3 \rangle = 4.873\ \mathrm{Im}\, \widetilde{d}_\tau^W + 1.505\ \mathrm{Re}\, \widetilde{d}_\tau^\gamma,$$
$$\langle \mathcal{O}_4 \rangle = 14.088\ \mathrm{Re}\, \widetilde{d}_\tau^W - 0.047\ \mathrm{Im}\, \widetilde{d}_\tau^\gamma.$$

- Six moments constrain all four components already on peak.
- A strong correlation remains: $\rho(\mathrm{Im}\, \widetilde{d}_\tau^W, \mathrm{Re}\, \widetilde{d}_\tau^\gamma) = -0.927$.

An energy scan changes the relative phase and separates the dipoles

Du, Zou, He and Xie, arXiv:2609.18892. Six-moment results from the manuscript revision.

A small off-peak scan improves dipole separation



- Keep 95% of the luminosity on peak. Share 5% equally at $m_Z \pm 1.7, \pm 3.5$ GeV.
- The real part of D^γ / D^Z changes sign across the resonance.

Fixed total luminosity. Only 1.2% of the tau pairs are off peak at this benchmark.

Du, Zou, He and Xie, arXiv:2609.18892. Six-moment results from the manuscript revision.

Projected joint sensitivity at FCC-ee and CEPC

Marginalized 1σ statistical uncertainties, six moments plus the 5% scan

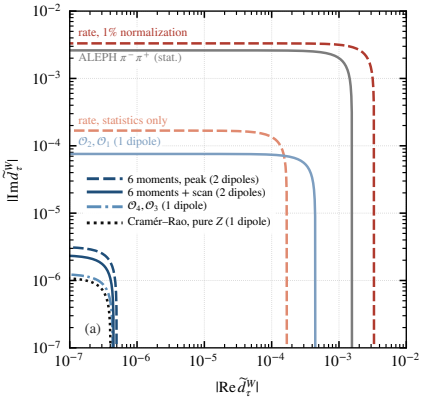
Component	FCC-ee	CEPC
$\mathrm{Re}\,\widetilde{d}_\tau^W$	$\mathbf{4.5\times10^{-7}}$	5.4×10^{-7}
$\mathrm{Im}\,\widetilde{d}_\tau^W$	$\mathbf{2.4\times10^{-6}}$	2.9×10^{-6}
$\mathrm{Re}\,\widetilde{d}_\tau^\gamma$	8.8×10^{-6}	1.1×10^{-5}
$\mathrm{Im}\,\widetilde{d}_\tau^\gamma$	2.0×10^{-5}	2.4×10^{-5}

$N_Z = 6.0\,(4.1)\times10^{12}$ at FCC-ee (CEPC), full angular acceptance, $\epsilon_\pi = 0.8$ per side. No radiation or angular-reconstruction simulation.

FCC-ee weak reach: 2.5×10^{-21} **and** $1.3\times10^{-20}\,e\,\mathrm{cm}$

Du, Zou, He and Xie, arXiv:2609.18892. Six-moment results from the manuscript revision.

Weak-dipole reach relative to published benchmarks



Weak dipoles

- The joint statistical forecast lies about three orders below ALEPH's published $\pi\pi$ statistical errors.
- Transverse moments preserve most of the relevant single-pion angular information.

The plotted arms illustrate tabulated 1σ errors on logarithmic axes. They are not joint confidence contours.

Du, Zou, He and Xie, arXiv:2609.18892. Six-moment results from the manuscript revision.

Experimental requirements for the statistical reach

- **Tau direction and pion azimuth**
  Impact parameters and beam constraints recover transverse spin information.
- **Angular acceptance and charge calibration**
  CP-symmetric selection protects the null mean. Acceptance still changes the response and covariance.
- **Radiation and beam-energy distribution**
  Initial-state radiation changes the photon–Z phase and must enter the scan model.

The modeled up/down charge asymmetry correlated with the forward/backward hemisphere needs control at roughly 2×10^{-5} for FCC-ee

Du, Zou, He and Xie, arXiv:2609.18892. Six-moment results from the manuscript revision.

Summary

Light axion-like particles

- Mono-γ and mono-Z searches probe ALPs that escape the detector.
- Nonresonant VBS extends the reach through virtual electroweak interactions.

Tau weak electric dipoles

- Transverse spin moments retain linear CP-odd interference.
- Six moments and a small scan separate both complex tau dipoles.

$$\boxed{\delta \operatorname{Re} \widetilde{d}_\tau^W = 4.5 \times 10^{-7}, \quad \delta \operatorname{Im} \widetilde{d}_\tau^W = 2.4 \times 10^{-6} \quad \text{(FCC-ee, statistical)}}$$

ALPs: Bao et al., arXiv:2505.10023. Tau dipoles: Du et al., arXiv:2609.18892 (six-moment revision). The two studies give complementary, independent probes.

Backup: collider benchmarks and references

ALP Tera-Z	$(87.9, 91.2, 94.3)$ GeV, $(40, 125, 40)\,\mathrm{ab}^{-1}$
ALP continuum	e^+e^-: 240/365 GeV. $\mu^+\mu^-$: 3/10 TeV. Contours compare $1, 5, 10\,\mathrm{ab}^{-1}$
Tau factories	$N_Z = 6.0 \times 10^{12}$ (FCC-ee), 4.1×10^{12} (CEPC)
Tau scan	95% luminosity on peak, 1.25% each at $m_Z \pm 1.7, \pm 3.5$ GeV

ALP study

Shou-shan Bao, Yang Ma, Yongcheng Wu, Keping Xie and Hong Zhang

Light axion-like particles at future lepton colliders, arXiv:2505.10023

Tau dipole study

Xin-Yu Du, Zi-Yue Zou, Xiao-Gang He and Keping Xie

Transverse Tau Spin Correlations and the Weak Electric Dipole Moment at Future Z Factories, arXiv:2609.18892

Results shown: updated six-moment analysis.

Backup: complete ALP electroweak matching

$$g_{a\gamma\gamma} = \frac{4}{f_a}(s_W^2 C_W + c_W^2 C_B),$$

$$g_{a\gamma Z} = \frac{8}{f_a} s_W c_W (C_W - C_B),$$

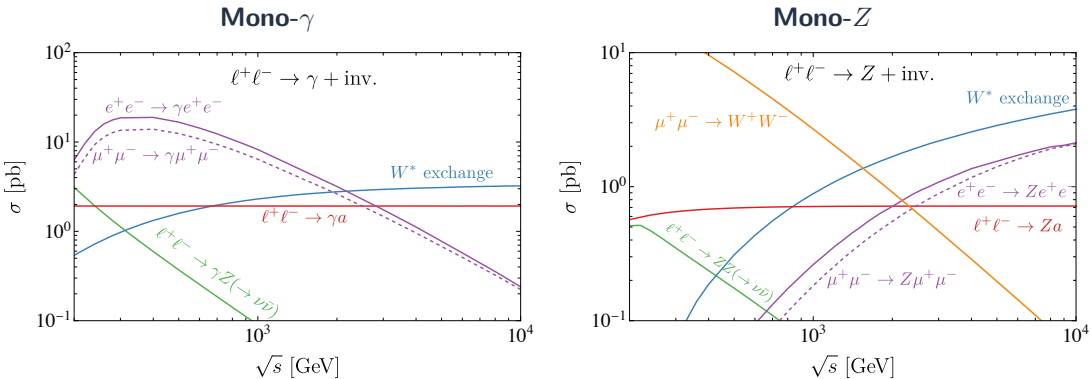
$$g_{aZZ} = \frac{4}{f_a}(c_W^2 C_W + s_W^2 C_B),$$

$$g_{aWW} = \frac{4}{f_a} C_W.$$

- The four mass-basis couplings arise from two electroweak coefficients.
- $C_W = C_B$ cancels the tree-level $a\gamma Z$ coupling in this convention.
- Combining channels reduces weakly constrained coefficient directions.

Bao, Ma, Wu, Xie and Zhang, arXiv:2505.10023.

Backup: mono-V production rates

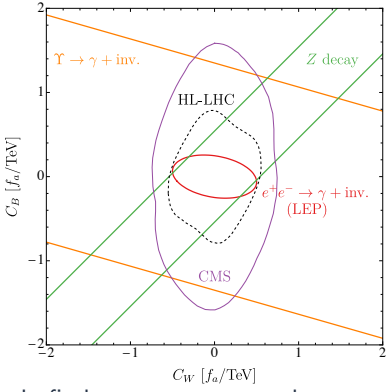


In the light-mass regime, signal rates vary weakly with m_a. The source mono-γ preselection uses $p_T^\gamma > 10$ GeV and $|\eta_\gamma| < 2.5$.

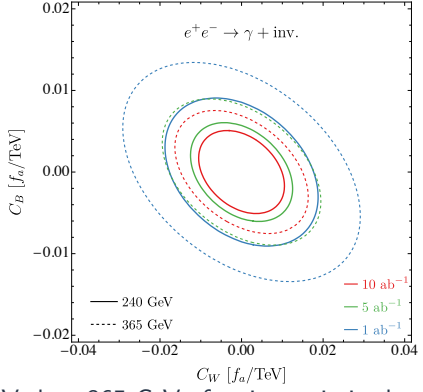
Bao, Ma, Wu, Xie and Zhang, arXiv:2505.10023.

Backup: existing constraints and electron mono-photon reach

Recast in the electroweak coefficient plane



e^+e^-: 240 and 365 GeV

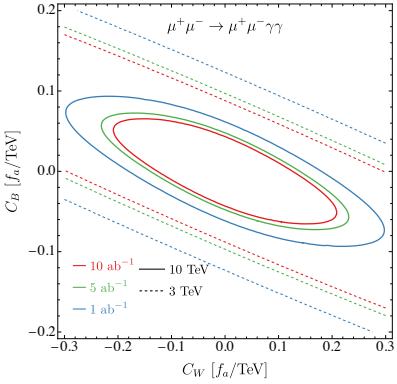


The study finds stronger mono-photon reach at 240 GeV than 365 GeV after its optimized selections.

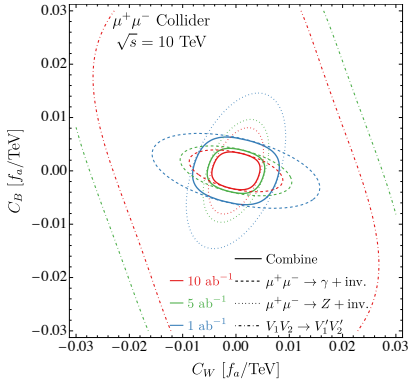
Bao, Ma, Wu, Xie and Zhang, arXiv:2505.10023.

Backup: light-by-light and electroweak VBS

Light-by-light scattering



Channel combination at 10 TeV

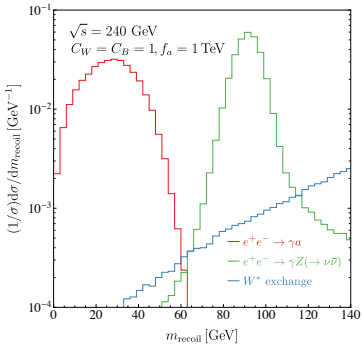


$\gamma\gamma \to \gamma\gamma$ probes the photonic direction. Weak-boson and mono-V channels provide complementary constraints.

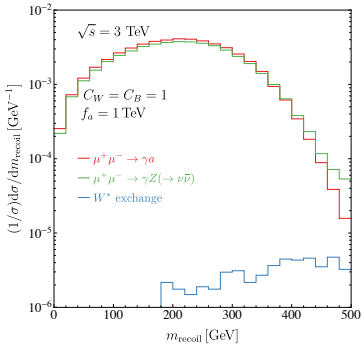
Bao, Ma, Wu, Xie and Zhang, arXiv:2505.10023.

Backup: recoil mass and mono-Z selections

Recoil mass at 240 GeV



Recoil mass at 3 TeV



- Mono-Z: $|M_{\ell\ell} - m_Z| < 10$ GeV or $|M_{\rm had} - m_Z| < 20$ GeV (resolved jj or one boosted jet).
- Optimized kinematic cuts suppress ZZ, WW and exchange backgrounds.

Bao, Ma, Wu, Xie and Zhang, arXiv:2505.10023.

Backup: near-optimal single-pion moments

Pure-Z, one nonzero weak-dipole component, independent pion measurements

FCC-ee benchmark	$\delta \operatorname{Re} \widetilde{d}_\tau^W$	$\delta \operatorname{Im} \widetilde{d}_\tau^W$
$\mathcal{O}_4$, $\mathcal{O}_3$	4.4×10^{-7}	1.3×10^{-6}
Classical Cramér–Rao bound	4.0×10^{-7}	1.1×10^{-6}
Excess uncertainty	8%	14%
Information efficiency	86%	77%

These moments retain most single-pion information

Classical, single-parameter benchmark. Percentages use unrounded errors.

Du, Zou, He and Xie, arXiv:2609.18892. Six-moment results from the manuscript revision.

Backup: analytical pole responses with photon interference

Define $D_v = \widetilde{d}_\tau^W + i\epsilon_v \widetilde{d}_\tau^\gamma$ and $D_a = \widetilde{d}_\tau^W + i\epsilon_a \widetilde{d}_\tau^\gamma$. At $s = m_Z^2$, with rows ordered $\mathcal{O}_1, \ldots, \mathcal{O}_6$,

$$\langle \boldsymbol{\mathcal{O}} \rangle_{\rm pole} \simeq -\frac{\beta}{\Delta_0} \begin{pmatrix} \frac{4}{3} v_\tau \ \mathrm{Im}\, D_v \\ \frac{4}{9} v_\tau \ \mathrm{Re}\, D_v \\ \frac{\pi}{2} h a_\tau A_e \beta \ \mathrm{Im}\, D_a \\ \frac{2}{3} h a_\tau \beta \ \mathrm{Re}\, D_v \\ \frac{\pi}{2} h v_\tau A_e \big(\mathrm{Re}\, D_a + \xi \ \mathrm{Im}\, \widetilde{d}_\tau^W \big) \\ \frac{2}{3} h v_\tau \ \mathrm{Im}\, D_v \end{pmatrix}.$$

$h = m_Z/(2m_\tau)$ and $\Delta_0 = 2a_\tau^2\beta^2 + v_\tau^2(3-\beta^2)$. Full angular acceptance, $\alpha_\pi = 1$, linear dipole response.

Dominant pole terms and indicated photon interference. The numerical joint fit retains additional interference terms.

Du, Zou, He and Xie, arXiv:2609.18892. Six-moment results from the manuscript revision.

Backup: interference coefficients and scope

$$\epsilon_v = \frac{\Gamma_Z}{m_Z}\frac{Q_e v_e}{v_e^2 + a_e^2} = 3.35 \times 10^{-3},$$

$$\epsilon_a = \frac{\Gamma_Z}{m_Z}\frac{Q_e}{2v_e} = 0.309,$$

$$\xi = \frac{\Gamma_Z}{m_Z}\frac{Q_e Q_\tau}{v_\tau A_e a_e} = 7.0, \qquad Q_e = Q_\tau = -1.$$

For $D_{v,a} = \widetilde{d}_\tau^W + i\epsilon_{v,a}\widetilde{d}_\tau^\gamma$,

$$\operatorname{Re} D_{v,a} = \operatorname{Re} \widetilde{d}_\tau^W - \epsilon_{v,a} \operatorname{Im} \widetilde{d}_\tau^\gamma,$$
$$\operatorname{Im} D_{v,a} = \operatorname{Im} \widetilde{d}_\tau^W + \epsilon_{v,a} \operatorname{Re} \widetilde{d}_\tau^\gamma.$$

Recover the pure-Z expressions by removing photon exchange. With $\widetilde{d}_\tau^\gamma = 0$ alone, the $\xi \operatorname{Im} \widetilde{d}_\tau^W$ term in $\mathcal{O}_5$ survives.

The full joint fit uses both propagators and retains the additional interference responses, including those needed for $\mathcal{O}_6$.

Du, Zou, He and Xie, arXiv:2609.18892. Six-moment results from the manuscript revision.

Backup: joint-fit covariance and pole responses

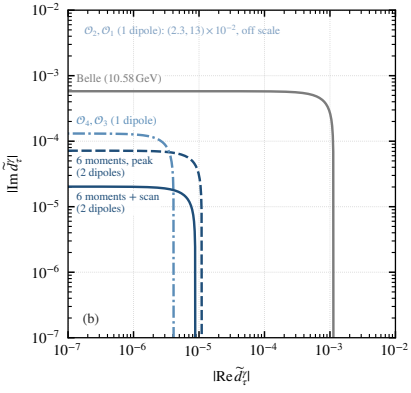
$$
\begin{aligned}
\langle \mathcal{O}_3 \rangle &= 4.873\ \mathrm{Im}\,\widetilde{d}_\tau^{W} + 1.505\ \mathrm{Re}\,\widetilde{d}_\tau^{\gamma}, \\
\langle \mathcal{O}_4 \rangle &= 14.088\ \mathrm{Re}\,\widetilde{d}_\tau^{W} - 0.047\ \mathrm{Im}\,\widetilde{d}_\tau^{\gamma}, \\
\langle \mathcal{O}_5 \rangle &= 0.360\ \mathrm{Re}\,\widetilde{d}_\tau^{W} + 2.508\ \mathrm{Im}\,\widetilde{d}_\tau^{W} - 0.111\ \mathrm{Im}\,\widetilde{d}_\tau^{\gamma}, \\
\langle \mathcal{O}_6 \rangle &= -0.0786\ \mathrm{Re}\,\widetilde{d}_\tau^{W} + 1.040\ \mathrm{Im}\,\widetilde{d}_\tau^{W} + 0.00348\ \mathrm{Re}\,\widetilde{d}_\tau^{\gamma} + 0.0485\ \mathrm{Im}\,\widetilde{d}_\tau^{\gamma}.
\end{aligned}
$$

$$
F = \sum_E R_E^T V_E^{-1} R_E, \qquad \mathrm{Cov}(\widehat{\boldsymbol{d}}) = F^{-1}, \qquad \boldsymbol{d} = (\mathrm{Re}\,\widetilde{d}_\tau^{W}, \mathrm{Im}\,\widetilde{d}_\tau^{W}, \mathrm{Re}\,\widetilde{d}_\tau^{\gamma}, \mathrm{Im}\,\widetilde{d}_\tau^{\gamma}).
$$

- R_E contains the linear moment responses. V_E is the full covariance of the estimated means.
- $N_{\mathrm{eff}}^{\mp} = N_Z B_Z B_\pi \epsilon$ and $N_{\mathrm{eff}}^{+-} = N_Z B_Z (B_\pi \epsilon)^2$.
- $B_Z = 0.033696$, $B_\pi = 0.1082$, $\epsilon = 0.8$ per pion side.

Du, Zou, He and Xie, arXiv:2609.18892. Six-moment results from the manuscript revision.

Backup: electromagnetic dipoles and published bounds



Published 95% CL bounds

ALEPH at $q^2 = m_Z^2$:

$$|\,\mathrm{Re}\,\widetilde{d}_\tau^W| < 0.91 \times 10^{-3},$$
$$|\,\mathrm{Im}\,\widetilde{d}_\tau^W| < 2.01 \times 10^{-3}.$$

Belle at $\sqrt{q^2} = 10.58$ GeV:

$$-1.10 < 10^3\,\mathrm{Re}\,\widetilde{d}_\tau^\gamma < 3.33,$$
$$-0.41 < 10^3\,\mathrm{Im}\,\widetilde{d}_\tau^\gamma < 1.86.$$

The forecast for $\mathrm{Re}\,\widetilde{d}_\tau^\gamma$ is about two orders below Belle's total uncertainty.

Relating different q^2 values requires a model, especially for light new particles.

Du, Zou, He and Xie, arXiv:2609.18892. Six-moment results from the manuscript revision.

Backup: rate information and normalization limits

Pure-Z benchmark with $\widetilde{d}_\tau^{\gamma} = 0$ and $N_0 = N_{\rm eff}^{+-}$:

$$\frac{N - N_0}{N_0} = A|\widetilde{d}_\tau^{W}|^2, \qquad A = 908.2.$$

$$\rho_{\rm stat} = \left(\frac{1}{A\sqrt{N_0}}\right)^{1/2}, \qquad \rho_{\rm sys} = \sqrt{\frac{\delta_N}{A}}.$$

FCC-ee benchmark	Radius in the complex $\widetilde{d}_\tau^{W}$ plane
Statistics only, 68.27% central count interval	1.7×10^{-4}
1% rate-normalization uncertainty	3.3×10^{-3}
0.3% rate-normalization uncertainty	1.8×10^{-3}

CP-odd normalized moments retain linear sensitivity and sign information

A rate radius is not a Gaussian component uncertainty.

Du, Zou, He and Xie, arXiv:2609.18892. Six-moment results from the manuscript revision.

Backup: selected references

- S.-s. Bao, Y. Ma, Y. Wu, K. Xie and H. Zhang,
  Light axion-like particles at future lepton colliders, arXiv:2505.10023.
- X.-Y. Du, Z.-Y. Zou, X.-G. He and K. Xie,
  Transverse Tau Spin Correlations and the Weak Electric Dipole Moment at Future Z Factories, arXiv:2609.18892
  Results shown: updated six-moment analysis..
- ALEPH, *Search for anomalous weak dipole moments of the tau lepton*,
  Eur. Phys. J. C **30** (2003) 291, hep-ex/0209066.
- Belle, *An improved search for the electric dipole moment of the τ lepton*,
  JHEP **04** (2022) 110, arXiv:2108.11543.
- J. Vidal, J. Bernabéu and G. González-Sprinberg,
  Tau weak dipole moments from azimuthal asymmetries, hep-ph/9812373.